International Journal of
Molecular Sciences

MDPI

Communication

Novel Class of Proteasome Inhibitors: In Silico and In Vitro Evaluation of Diverse Chloro(trifluoromethyl)aziridines

Laura Ielo [1], Vincenzo Patamia [2], Andrea Citarella [3], Thomas Efferth [4], Nasim Shahhamzehei [4], Tanja Schirmeister [5], Claudio Stagno [3], Thierry Langer [6], Antonio Rescifina [2], Nicola Micale [3] and Vittorio Pace [1,6,*]

1 Department of Chemistry, University of Turin, Via P. Giuria 7, 10125 Torino, Italy
2 Dipartimento di Scienze del Farmaco e della Salute, University of Catania, Viale A. Doria 6, 95125 Catania, Italy
3 Department of Chemical, Biological, Pharmaceutical and Environmental Sciences, University of Messina, Viale Ferdinando Stagno D'Alcontres 31, 98166 Messina, Italy
4 Department of Pharmaceutical Biology, Institute of Pharmaceutical and Biomedical Sciences, Johannes Gutenberg University, Staudinger Weg 5, 55128 Mainz, Germany
5 Department of Medicinal Chemistry, Institute of Pharmaceutical and Biomedical Sciences, Johannes Gutenberg University, Staudinger Weg 5, 55128 Mainz, Germany
6 Department of Pharmaceutical Sciences, Division of Pharmaceutical Chemistry, University of Vienna, Josef-Holaubek-Platz 2, 1090 Vienna, Austria
* Correspondence: vittorio.pace@unito.it or vittorio.pace@univie.ac.at; Tel.: +39-011-670-7934

Abstract: The ubiquitin-proteasome pathway (UPP) is the major proteolytic system in the cytosol and nucleus of all eukaryotic cells. The role of proteasome inhibitors (PIs) as critical agents for regulating cancer cell death has been established. Aziridine derivatives are well-known alkylating agents employed against cancer. However, to the best of our knowledge, aziridine derivatives showing inhibitory activity towards proteasome have never been described before. Herein we report a new class of selective and nonPIs bearing an aziridine ring as a core structure. In vitro cell-based assays (two leukemia cell lines) also displayed anti-proliferative activity for some compounds. In silico studies indicated non-covalent binding mode and drug-likeness for these derivatives. Taken together, these results are promising for developing more potent PIs.

Keywords: proteasome inhibitors; aziridines; computational studies; in vitro assays; anti-proliferative activity

Citation: Ielo, L.; Patamia, V.; Citarella, A.; Efferth, T.; Shahhamzehei, N.; Schirmeister, T.; Stagno, C.; Langer, T.; Rescifina, A.; Micale, N.; et al. Novel Class of Proteasome Inhibitors: In Silico and In Vitro Evaluation of Diverse Chloro(trifluoromethyl)aziridines. *Int. J. Mol. Sci.* **2022**, *23*, 12363. https://doi.org/10.3390/ijms232012363

Academic Editor: Hanoch Senderowitz

Received: 13 September 2022
Accepted: 11 October 2022
Published: 15 October 2022

1. Introduction

The dynamic conditions of intracellular proteins are preserved by a perfect equilibrium between protein synthesis and degradation. Thus, the quality and quantity of proteins within a cell must be strictly regulated according to cellular needs or physiological demands. In this regard, the ubiquitin-proteasome pathway (UPP) constitutes the major proteolytic system in the cytosol and nucleus of all eukaryotic cells. It is crucial for maintaining intracellular protein homeostasis in physiological conditions and during adaptive stress responses [1–5]. UPP catalyzes the degradation of most short-lived and long-lived proteins, which comprehend the number of proteins in mammalian cells [6,7]. The degradation of proteins by the UPP is a cyclic pathway involving an initial step of ubiquitin (Ub) conjugation to the protein substrate, resulting in the degradation of the polyubiquitinated protein via the 26S proteasome complex [5,8–10]. The eukaryotic 26S proteasome is a large (~2.5 MDa) multifunctional particle, composed of a barrel-shaped 20S core particle (CP), which contains the protease subunits, capped by two 19S regulatory particles (RPs) that control the proteolytic function of the protease core. The 20S proteasome is the proteolytically active key component of the ubiquitin-proteasome system. It is constituted by four heptameric rings stacked in a α7β7β7α7 arrangement. The two inner β-rings

contain the proteolytic active sites (β1–7). In particular, the three proteolytic subunits are β1, β2, and β5, which have distinct substrate specificities [11–13]. β5 subunits display "chymotrypsin-like" (ChT-L) activity and are mainly involved in protein degradation. Therefore, they emerged as the principal targets for developing efficacious anticancer agents [14,15]. The other two proteolytic subunits of the proteasome, β2 and β1, must be considered as co-targets of anticancer agents to achieve an efficient protein breakdown. β2 subunits possess "trypsin-like" (T-L) activity, whereas β1 subunits are referred to as "post-glutamate peptide hydrolase" (PGPH) or "caspase-like" (C-L) [13,16,17]. All three catalytic subunits contain an *N*-terminal residue, Thr1, of which the hydroxyl group acts as a nucleophile and interacts with the peptides of the proteins to be degraded [16,18,19]. Immediately after the disclosure of the UPP and its relevance to protein and cellular homeostasis, preclinical studies on the presumed role of proteasome inhibitors (PIs) as critical agents for regulating cancer cell death have commenced [20,21]. The proteasome was identified and validated as a pivotal target in protein quality control and turnover, cell differentiation, cell-cycle regulation, and apoptosis [5,8–10,22]. To date, three PIs have been approved by the US Food and Drug Administration Agency (FDA) and the European Medicine Agency (EMA), Velcade® (bortezomib, **2**) [23,24], Ninlaro® (ixazomib, **3**) [23], and Kyprolis® (carfilzomib, **6**) [23] (Figure 1), as new drugs to treat multiple myeloma (MM) and mantle-cell lymphoma (MCL). It is known that the co-inhibition of the β5 subunits with either the β1 or the β2 subunits provides the maximal anti-tumor effect and represents the ideal profile for a drug candidate [25–27]. On the contrary, the inhibition of all proteasome subunits may develop cytotoxicity [28]. The majority of 20S PIs currently reported in literature [2,29–31], are peptide-based compounds, featured with a *C*-terminal electrophilic warhead that forms covalent adducts with the hydroxyl group of Thr1 in the active sites. A reversible mechanism of action is observed for aldehydes (**1**) [3,32–34], boronates (**2–3**) [23,24,35–37], α-keto-amides (**4**) [37,38], and α-keto-aldehydes (**5**) [39]. α′,β′-Epoxyketones (**6**) [3,34,40], β-lactones (**7**) [41,42], vinyl sulfones (**8**) [43–45], vinyl esters (**9**) [46], and syrabactins (**10**) [47] act as irreversible inhibitors (Figure 1a) [2]. For the latter, the covalent mode of action and the elevated reactivity of the compounds may often lead to off-target interactions. Lately, diverse new non-covalent PIs were identified (Figure 1b) [17,48–52]. Even if less widely investigated with respect to covalent inhibitors, they provide a valid and milder alternative mechanism for proteasome inhibition.

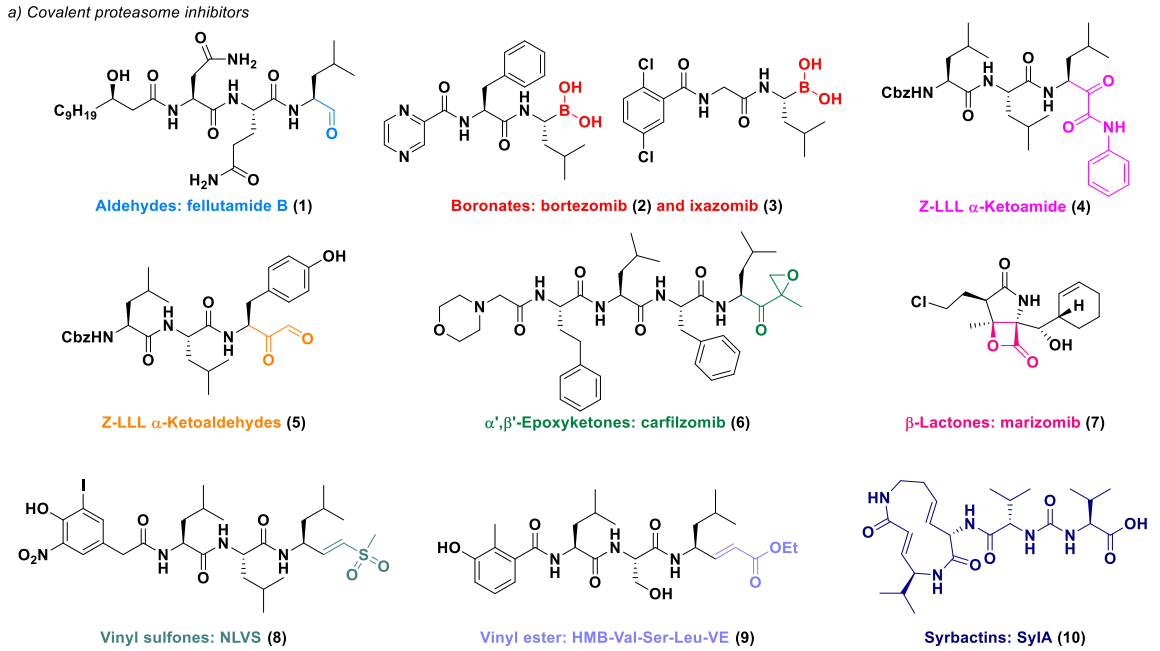

Figure 1. *Cont.*

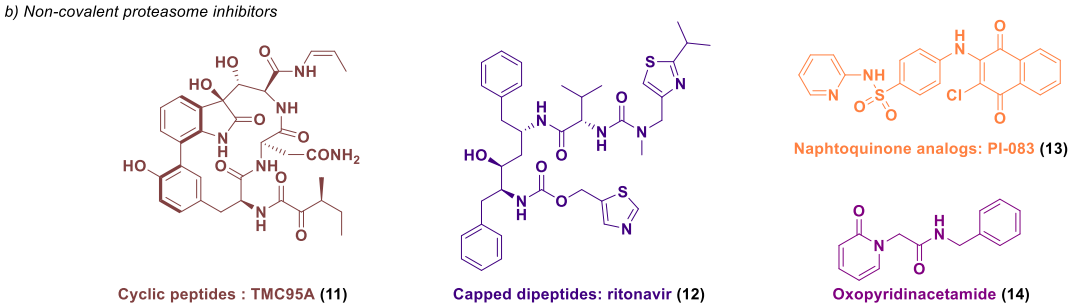

Figure 1. Representative examples of the major classes of covalent (**a**) and non-covalent (**b**) PIs from natural and synthetic sources.

2. Results and Discussion

Despite the remarkable achievements in obtaining PIs, further research is still needed due to the lack of selectivity and resistance development of the inhibitors and drugs reported so far. Recently, we discovered a new class of aziridine featuring compounds as promising PIs. Albeit aziridine derivatives are well-known alkylating agents employed against cancer [53–55], to the best of our knowledge, aziridine derivatives showing inhibitory activity towards proteasome have never been reported. Thus, inspired by in silico predictions (see hereinafter), the in vitro biological activity of selected chloro (trifluoromethyl)aziridines (CTMAs) (Scheme 1), synthesized by Ielo et al. in 2019 [56], was evaluated toward human 20S proteasome. CTMAs were synthesized via homologation chemistry enriched with a brand-new interesting biological applicability in the field of drug discovery, as already evidenced by our research group activity [57–60]. The investigation started by performing docking studies using proteasome β5 subunit of *Saccharomyces cerevisiae* (PDB ID: 4HRD) [61] in order to assess possible binding modes of CTMAs to the catalytic pocket of the target. The peptide Suc-Leu-Leu-Val-Tyr-AMC (**26**, Figure 2a) was used as a reference proteasome substrate. Docking results predicted promising activities as PIs (Table 1). With these results in hand, we decided to evaluate the in vitro inhibitory activity of compounds **15–25** against the ChT-L activity of the human 20S proteasome [31,44,62–66]. The calculated free energies of binding (Δ*G*) and the calculated and experimental Ki values at the binding site of the proteasome are reported in Table 1.

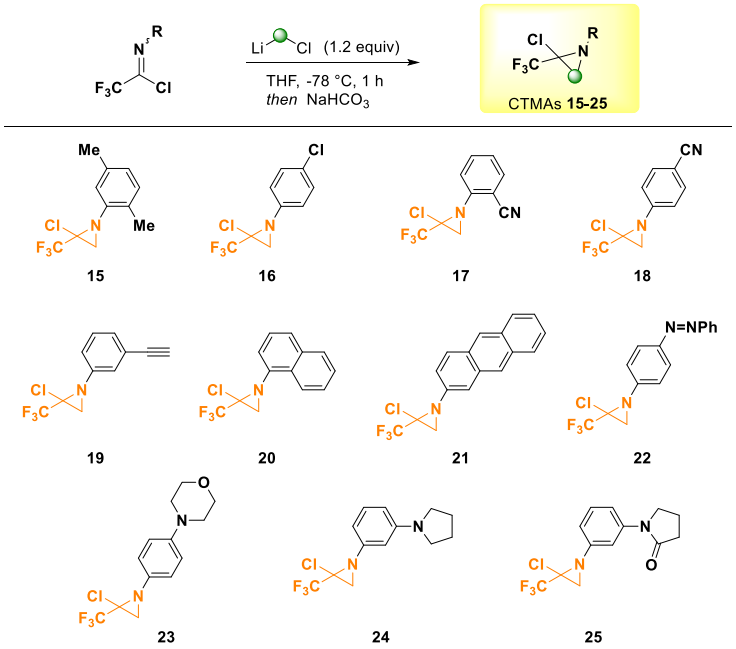

Scheme 1. Chemical structure of chloro(trifluoromethyl)aziridines (CTMAs, **15–25**).

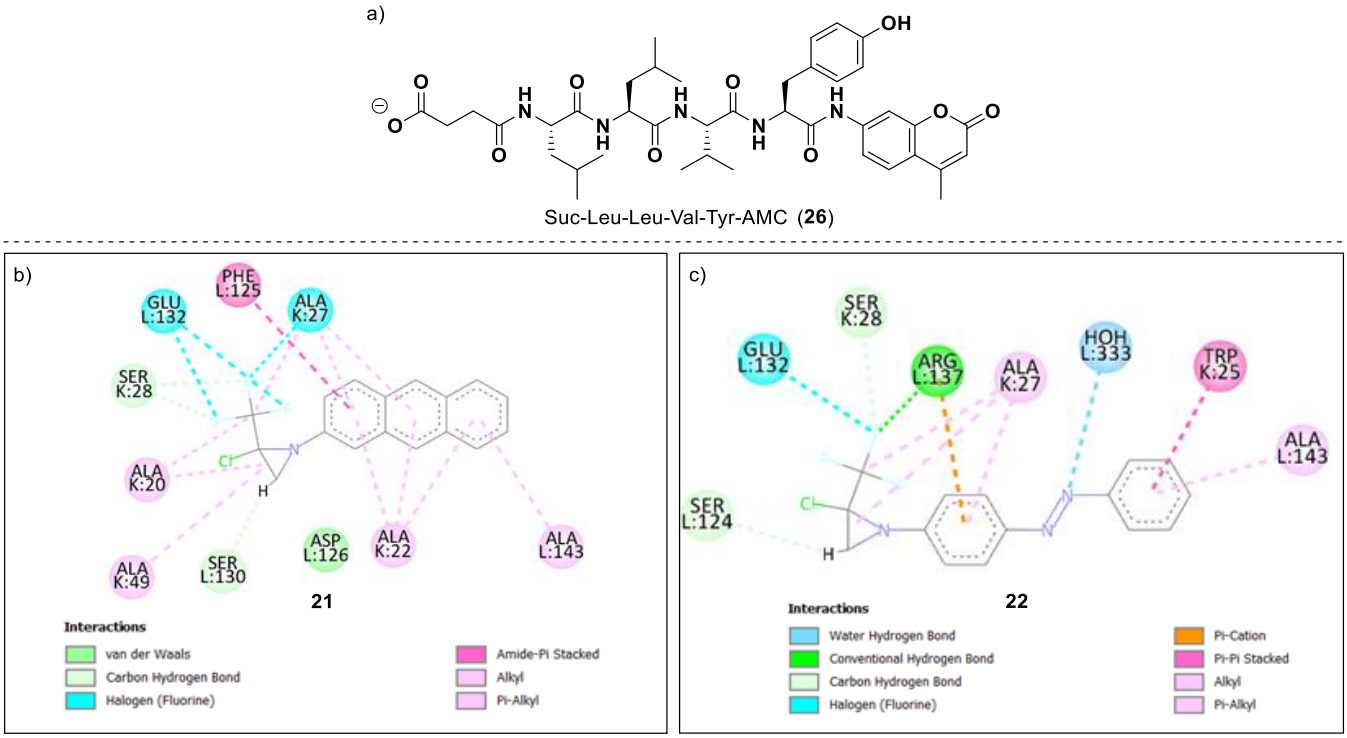

Figure 2. Reference compound structure Suc-Leu-Leu-Val-Tyr-AMC (**26**) is used as the positive control (**a**). The 2D poses of CTMAs **21** (**b**) and **22** (**c**), respectively, within the receptor pocket.

Table 1. Docking scores, predicted K_i on proteasome β5 subunit of *Saccharomyces Cerevisiae* (PDB ID: 4HRD), and inhibitory activity of compounds **15**–**25** compared to that of reference **26**.

Compound	Δ*G* Vina	K_i Calc. (μM)	ChT-L Activity (% Inhibition at 20 μM) [1]	IC_{50}/K_i (μM) ChT-L [2]
15	−6.91	8.56	<20	-
16	−7.18	5.42	25 ± 1.1	-
17	−7.07	6.53	<20	-
18	−7.64	2.49	37 ± 0.5	-
19	−7.40	3.74	<20	-
20	−7.89	1.64	<20	-
21	−8.31	0.80	68 ± 0.4	13.6 ± 1.1/1.6 ± 0.13
22	−8.59	0.50	67 ± 0.1	14.1 ± 0.7/1.6 ± 0.08
23	−7.88	1.66	41 ± 1.2	-
24	−7.85	1.75	27 ± 0.3	-
25	−8.11	1.31	34 ± 1.4	-
26	−8.75	0.38	-	-

[1] Screening assays on human 20S proteasome ChT-L activity (β5 subunit). [2] Continuous assays on human 20S proteasome ChT-L activity (β5 subunit) with final inhibitor concentrations 0, 2.5, 5, 10, 20, 30, 40, and 50 μM performed for 30 min only for compounds that showed >60% of inhibition in the screening test. IC_{50} values include standard deviation from two independent experiments, each performed in duplicate. K_i ± SD values have been calculated using the Cheng-Prusoff equation. The K_m values were determined in separate experiments: For ChT-L activity with Suc-Leu-Leu-Val-Tyr-AMC K_m = 13 μM.

Screening assays against human 20S proteasome ChT-L activity (β5 subunit) were performed for all CTMAs (**15**–**25**) at a concentration of 20 μM using DMSO (Dimethyl Sulfoxide) as a negative control [67]. The two most active CTMAs (i.e., **21** and **22**) showed inhibitory activity of 68% and 67%, respectively, suggesting that bulky hydrophobic groups at the aziridine nitrogen are preferred for effective binding to the target. Therefore, they were selected for continuous assays providing IC_{50} values of 13.6 and 14.1 μM, respectively, and binding affinity (Ki) in the low-micromolar range (Table 1).

Preliminary assays (i.e., screening at 20 μM) carried out on several cysteine and serine proteases, as well as on proteasome β1 and β2 subunits, did not show any inhibitory activity (inhibition range 0–5%), indicating a marked selectivity of compounds **15**–**25** towards proteasome β5 subunits. Afterwards, we moved to cell-based assays to assess a correlation between the proteasome ChT-L inhibition and the anti-proliferative activity of CTMAs by using the resazurin method on two different leukemia cells lines (Table 2) [68–70]. Derivatives **21** and **22** displayed the best anti-proliferative profile also in this assay with an IC_{50} value of 25.45 and 32.82 μM on CCRF-CEM (drug-sensitive acute lymphocytic leukemia cells) and of 24.08 and 67.72 μM on CEM/ADR500 (multidrug-resistant leukemia sub-cell line) [71–73], respectively. Noteworthy, both **21** and **22** didn't show cytotoxicity against healthy peripheral blood mononuclear cells (PBMCs) (Table 2) (Figure S1).

Table 2. Cytotoxicity of compounds **15**–**25** towards drug-sensitive acute lymphocytic leukemia cells (CCRF-CEM), multidrug-resistant leukemia sub-cell line (CEM/ADR5000), and healthy peripheral blood mononuclear cells (PBMCs) using the resazurin reduction assay. All values are shown as mean ± standard deviation (SD) of three independent experiments. The degree of resistance was calculated by dividing the IC_{50} value of resistant by that of sensitive cells.

Compound	CCRF-CEM IC_{50} (μM)	CEM/ADR5000 IC_{50} (μM)	PBMCs CC_{50} (μM)	Degree of Resistance
15	>100	>100	-	-
16	55.03 ± 1.33	>100	-	-
17	>100	>100	-	-
18	>100	>100	-	-
19	>100	>100	-	-
20	>100	>100	-	-
21	25.45 ± 4.08	24.08 ± 4.05	>100	0.95
22	32.82 ± 1.28	67.72 ± 8.80	>100	2.06
23	56.95 ± 2.20	>100	-	-
24	42.15 ± 1.86	>100	-	-
25	82.41 ± 3.50	67.97 ± 3.20	-	0.82
Doxorubicin	0.044 ± 0.01	20.50 ± 2.59	-	463.90

In silico studies were performed using AutoDock Vina implemented in the YASARA software. The docking studies were performed on all the protonation states of the compounds at pH 7.4, previously calculated using the Marvin software. Following in silico studies, it was seen that the CTMAs tested can bind the receptor non-covalently and nevertheless possess a good inhibitory capacity. Considering CTMAs SAR (Structure-Activity Relationships), the phenyl ring substitution seems favorable in para-position since a decrease or even loss of activity was observed in derivatives substituted in ortho-position. Linear conjugated π systems, such as anthracene (**21**) and diazo-diphenyl (**22**), confer the best activity. The 2D structures for the two most active CTMAs, **21** and **22**, are shown in Figure 2b,c, respectively. CMTAs **21** and **22** establish somewhat similar interactions within the receptor site. From the 2D poses of the two compounds, it can be seen that both ligands establish hydrophobic interactions with the residues Ala27, Glu132, Ser28, and Ala143. The presence of a greater hydrophobic portion due to the anthracene moiety (**21**) allows the compound **21** to establish π-alkyl interactions with the Ala22 residue (Figure 2b). CTMA **22**, due to the presence of the two central nitrogen atoms, establishes a hydrogen bond (2.57 Å) with a water molecule inside the receptor site (Figure 2c). In addition, we performed in silico ADMET studies on CTMAs **21** and **22** to further strengthen the results of the docking studies. The ability to reach targets in bioactive form was evaluated using the SwissADME web platform (http://swissadme.ch, accessed on 15 July 2022). Notably, the technologies implemented in this platform can predict the false positive results commonly observed in biochemical small molecule assays with a fair degree of certainty. The two compounds simultaneously satisfy Lipinski's [74] and Veber's [75] rule for drug similarity. Both have a Bioavailability Score of 0.55. Importantly, CTMA **21** showed no alerts on the outcome

of the PAINS model of pan assay interference structures [76], designed to exclude small molecules that might show false positives in bioassays.

Human gastrointestinal uptake (HIA) and blood-brain barrier (BBB) penetration, related to absorption and distribution parameters, respectively, were graphically represented by the extended and revamped version of the Edan-Egg model, called the Brain Or IntestinaL EstimateD (BOILED) predictive permeation model (BOILED-Egg). Visual analysis of Figure 3 shows that CTMA **22** is passively absorbed by the gastrointestinal tract, and could be effluated from the central nervous system (CNS) with the aid of the P-glycoprotein. None of them was predicted to passively permeate through the BBB.

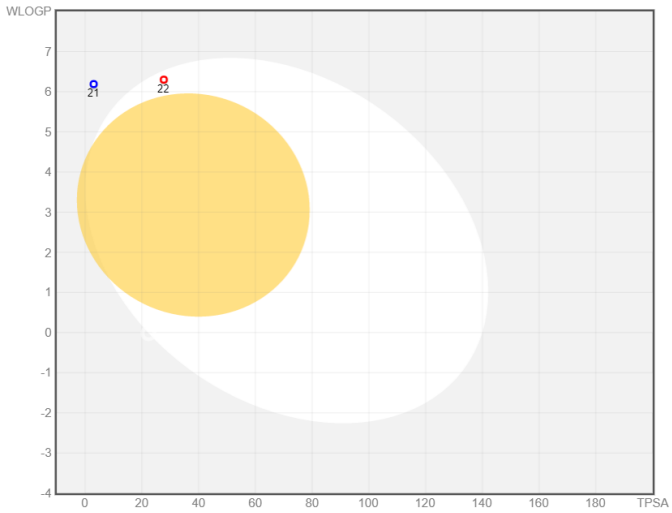

Figure 3. BOILED-Egg plot. Points located in the BOILED-Egg's yolk (yellow) represent the molecules predicted to passively permeate through the blood-brain barrier, whereas the ones in the egg white are relative to the molecules predicted to be passively absorbed by the gastrointestinal tract; the blue dots (**21**) indicate the molecules for which it was expected to be effluated from the CNS by the P-glycoprotein, whereas the red ones (**22**) point to the molecules predicted not to be effluated from the CNS by the P-glycoprotein.

3. Materials and Methods

3.1. General Methods

Melting points were determined on a Reichert–Kofler hot-stage microscope and are uncorrected. Mass spectra were obtained on a Shimadzu QP 1000 instrument (EI, 70 eV) and on a Bruker maXis 4G instrument (ESI-TOF, HRMS). ^{1}H, ^{13}C, ^{19}F, and ^{15}N NMR spectra were recorded with a Bruker Avance III 400 spectrometer (400 MHz for ^{1}H, 100 MHz for ^{13}C, 377 MHz for ^{19}F, 40 MHz for ^{15}N) and with a Bruker DRX spectrometer (200 MHz for ^{1}H, 50 MHz for ^{13}C) at 297 K. The center of the solvent signal was used as an internal standard which was related to TMS with δ 7.26 ppm (^{1}H in $CDCl_3$), δ 77.00 ppm (^{13}C in $CDCl_3$). ^{15}N NMR spectra were referenced against external nitromethane (0.0 ppm), ^{19}F NMR spectra by absolute referencing via $\in$ ratio. Spin-spin coupling constants (J) are given in Hz. In nearly all cases, complete and unambiguous assignment of all resonances was performed by applying standard NMR techniques, such as APT, HSQC, HMBC, COSY, and NOESY experiments.

THF was distilled over Na/benzophenone. Chemicals were purchased from Sigma-Aldrich, Acros, Alfa Aesar, Fluorochem, and TCI Europe, otherwise specified. Organolithium reagents were kindly provided by Albemarle Corporation. Solutions were evaporated under reduced pressure with a rotary evaporator. TLC was carried out on aluminum sheets precoated with silica gel 60F254 (Macherey-Nagel, Merck, Darmstadt, Germany); the spots were visualized under UV light (λ = 254 nm) and/or $KMnO_4$ (aq.) was used as a revealing system. Neutral Aluminium Oxide-Brockmann grade 2 (Alox-BG2) for chro-

matographic purifications was prepared as we previously reported [77]. MeLi-LiBr (1.5 M ethereal solution) was titrated immediately prior to use, according to the literature [78].

3.2. General Procedures

3.2.1. General Procedure for Preparing Trifluoroacetimidoyl Chlorides [79]

To a solution of Ph_3P (3.0 equiv) in DCE was added CCl_4 (4.0 equiv), Et_3N (1.2 equiv), and TFA (1.0 equiv) at 0 °C and the mixture was stirred for 10 min. After the solution was cooled to room temperature, suitable aniline (1.0 equiv) was added. The mixture was then refluxed overnight. The solvent was removed under reduced pressure, and the residue was diluted and washed with *n*-hexane several times and filtered. The filtrate was concentrated under reduced pressure, and the so-obtained crude mixture was subjected to chromatography (silica gel) to afford pure compounds.

3.2.2. General Procedure for Preparing Chloro-Trifluoromethylaziridines (CTMAs) [56]

To a cooled (−78 °C) solution of trifluoromethylchloroimidate (1.0 equiv) in dry THF was added chloroiodomethane (1.3 equiv). After 2 min, an ethereal solution of MeLi-LiBr (1.2 equiv, 1.5 M) was added dropwise using a syringe pump (flow: 0.200 mL/min). The resulting solution was stirred for 1 h. Then 10% aq solution $NaHCO_3$ (2 mL/mmol substrate) was added, and the reaction mixture was extracted with Et_2O (2 × 5 mL) and washed with water (5 mL) and brine (10 mL). The organic phase was dried over anhydrous Na_2SO_4, filtered, and, after removal of the solvent under reduced pressure, the so-obtained crude mixture was subjected to chromatography (Alox-BG2) to afford pure compounds.

3.3. In Silico Studies

The studied molecules were drawn using Marvin Sketch and minimized toward molecular mechanics by Merck molecular force field (MMFF94) optimization using the Marvin Sketch geometrical descriptors plugin. The protonation states of the molecules were calculated assuming a 7.4 pH. The MMFF91 obtained 3D structures were subsequently optimized using the parameterized model number 6 semi-empirical Hamiltonian with the corrections to hydrogen bonding and dispersion (PM6-D3H4) implemented in the MOPAC package (vMOPAC2016). Docking calculations were made using AutoDock Vina, as implemented in the YASARA package, with the default docking parameters. The X-ray crystal structures of the co-crystal proteasome subunit β5/Carmaphycin B (PDB ID: 4HRD) were downloaded from the Protein Data Bank (www.rcsb.org). Only chains K and L were used. Water molecules were also removed. All amino acid residues were kept rigid, whereas all single bonds of ligands were treated as fully flexible for both proteins. A 10 Å simulation cell around all atoms of the co-crystallized ligand was used. AMBER 14 force field was used for the simulation.

3.4. Biological Assays

3.4.1. Inhibition Assay for the Chymotrypsin-like Activity of the 20S Proteasome

The inhibitory activity of the compounds was evaluated by a standard fluorometric method [67]. Human 20S proteasome was obtained from a commercial source (Biomol GmbH, Hamburg, Germany), as well as the peptidic substrate (Bachem, Bubendorf, Switzerland) Suc-Leu-Leu-Val-Tyr-AMC·HCl for the chymotrypsin-like (ChT-L) activity of the enzyme. The proteolytic activity of the 20S proteasome was measured by monitoring the hydrolysis of the substrate by detecting the fluorescence of the product released, 7-amino-4-methyl coumarin (7-AMC), by means of an Infinite 200 PRO microplate reader (Tecan, Männedorf, Switzerland) at 30 °C with a 380 nm excitation filter and a 460 nm emission filter. Human 20S proteasome was employed for testing at a final concentration of 0.004 $mg \cdot mL^{-1}$ together with the fluorogenic substrate (100 μM) and compounds present at 20 μM (screening assay) or at variable concentrations (continuous assay). DMSO was used as a negative control. The reaction buffer consisted of 50 mM Tris pH 7.5, 10 mM NaCl, 25 mM KCl, 1 mM $MgCl_2 \cdot 6H_2O$, 0.03% SDS and 5% DMSO. The compounds and

enzyme were incubated for 30 min at 30 °C prior to substrate addition. Product release from substrate hydrolysis was monitored continuously for 10 min.

3.4.2. Inhibition Assay for the Post-Glutamyl Peptide Hydrolyzing (PGPH or Caspase-like) Activity of the 20S Proteasome

The assay against the caspase-like (Casp-L) activity of the human 20S proteasome was performed in the same experimental conditions as for the ChT-L activity. The enzyme employed for testing was incubated at a final concentration of 0.003 mg·mL^{-1} together with the appropriate fluorogenic substrate Z-Leu-Leu-Glu-AMC·HCl (80 µM) and compounds present at 20 µM (screening assay) or at variable concentrations (continuous assay). DMSO was used as a negative control. The reaction buffer consisted of 50 mM Tris pH 7.5, 10 mM NaCl, 25 mM KCl, 1 mM $MgCl_2 \cdot 6H_2O$, 0.03% SDS and 5% DMSO.

3.4.3. Inhibition Assay for Trypsin-like Activity of the 20S Proteasome

The assay against the trypsin-like (T-L) activity of the human 20S proteasome was performed in the same experimental conditions as for the ChT-L and Casp-L activity. The enzyme employed for testing was incubated at a final concentration of 0.0025 mg·mL^{-1} together with the appropriate fluorogenic substrate Boc-Leu-Arg-Arg-AMC·HCl (85 µM) and compounds present at 20 µM (screening assay) or at variable concentrations (continuous assay). DMSO was used as a negative control. The reaction buffer consisted of 50 mM Tris pH 7.4, 50 mM NaCl, 0.5 mM EDTA, 0.03% SDS and 5% DMSO.

3.4.4. Cell Culture

Drug-sensitive CCRF-CEM and multidrug-resistant (MDR) P-glycoprotein (P-gp)-over-expressing CEM/ADR5000 leukemic cells were kindly provided by Prof. Axel Sauerbrey (Department of Pediatrics, University of Jena, Germany). Cells were cultured in RPMI 1640 medium, including 10% fetal bovine serum (FBS) and 1% penicillin (1000 U mL^{-1})/streptomycin (100 mg mL^{-1}) (Life Technologies, Darmstadt, Germany). Doxorubicin (5000 ng mL^{-1}) was added to the culture medium to maintain overexpression of P-gp (MDR1/ABCB1) in CEM/ADR5000 cells every 14 days. The MDR-phenotype of CEM/ADR5000 cells has been characterized [71–73]. In vitro antiproliferative activity against CCRF-CEM and CEM/ADR5000 cell lines. The cytotoxic effects of the compounds in dimethyl sulfoxide (DMSO) were tested using a resazurin assay [68,69]. This assay is based on the reduction of the indicator dye, resazurin, to the highly fluorescent resorufin by viable cells [70]. The aliquot of 1×10^4 cells per mL cells was seeded into 96-well plates and immediately treated with various concentrations of each compound. After 72 h of incubation at 37 °C, 20 µL resazurin 0.01% w/v solution was added to each well, and the plates were maintained at 37 °C for 4 h. Fluorescence was measured using an Infinite M2000 Pro-plate reader (Tecan, Crailsheim, Germany) with an excitation wavelength of 544 nm and an emission wavelength of 590 nm. Each experiment was done at least three times with six replicates each. The viability was analyzed in comparison with the untreated cells. Fifty percent inhibition (IC_{50}) values are the drug concentrations required to inhibit 50% of cell proliferation and were calculated from a calibration curve by linear regression using Microsoft Excel.

4. Conclusions

In conclusion, a new class of non-covalent, selective, and not cytotoxic PIs has been described. The reported in silico and in vitro studies indicated the presence of promising derivatives within this class of compounds, leading the way for further optimization in order to develop more potent inhibitors.

Supplementary Materials: The following supporting information can be downloaded at: https://www.mdpi.com/article/10.3390/ijms232012363/s1.

Author Contributions: Conceptualization, L.I., A.R., V.P. (Vittorio Pace) and N.M.; methodology, L.I., A.C., C.S. and V.P. (Vincenzo Patamia); software, A.R., V.P. (Vittorio Pace) and T.L.; validation, T.E., T.S. and N.S.; formal analysis, L.I., A.C., C.S. and N.S.; investigation, L.I., A.C., V.P. (Vincenzo Patamia) and N.M.; resources, V.P. (Vittorio Pace), T.E., T.S., T.L. and A.R.; data curation, L.I., A.C., A.R., N.M., V.P. (Vincenzo Patamia) and T.E.; writing—original draft preparation, L.I., V.P. (Vincenzo Patamia) and A.C.; writing-review and editing, V.P. (Vittorio Pace), A.R. and N.M.; visualization, L.I., N.M., A.R. and V.P. (Vittorio Pace); supervision, V.P. (Vittorio Pace), A.R. and N.M.; project administration, L.I., V.P. (Vittorio Pace), A.R. and N.M.; funding acquisition, V.P. (Vittorio Pace), T.E., T.S., T.L. and N.M. All authors have read and agreed to the published version of the manuscript.

Funding: This research received no external funding.

Institutional Review Board Statement: Not applicable.

Informed Consent Statement: Not applicable.

Data Availability Statement: The data that support the findings of this study are available from the corresponding authors upon reasonable request.

Acknowledgments: The authors thank the University of Vienna, the University of Torino, and the University of Mainz for financial support. All4Labels Group (Hamburg, Germany) is acknowledged for generous funding.

Conflicts of Interest: The authors declare no conflict of interest.

References

1. Hershko, A.; Ciechanover, A. The ubiquitin system. *Annu. Rev. Biochem.* **1998**, *67*, 425–479. [CrossRef] [PubMed]
2. Leonardo-Sousa, C.; Carvalho, A.N.; Guedes, R.A.; Fernandes, P.M.P.; Aniceto, N.; Salvador, J.A.R.; Gama, M.J.; Guedes, R.C. Revisiting Proteasome Inhibitors: Molecular Underpinnings of Their Development, Mechanisms of Resistance and Strategies to Overcome Anti-Cancer Drug Resistance. *Molecules* **2022**, *27*, 2201. [CrossRef]
3. Kisselev, A.F.; Goldberg, A.L. Proteasome inhibitors: From research tools to drug candidates. *Chem. Biol.* **2001**, *8*, 739–758. [CrossRef]
4. Thompson, S.J.; Loftus, L.T.; Ashley, M.D.; Meller, R. Ubiquitin-proteasome system as a modulator of cell fate. *Curr. Opin. Pharmacol.* **2008**, *8*, 90–95. [CrossRef]
5. Bhat, K.P.; Greer, S.F. Proteolytic and non-proteolytic roles of ubiquitin and the ubiquitin proteasome system in transcriptional regulation. *Biochim. Biophys. Acta* **2011**, *1809*, 150–155. [CrossRef] [PubMed]
6. Rock, K.L.; Gramm, C.; Rothstein, L.; Clark, K.; Stein, R.; Dick, L.; Hwang, D.; Goldberg, A.L. Inhibitors of the proteasome block the degradation of most cell proteins and the generation of peptides presented on MHC class I molecules. *Cell* **1994**, *78*, 761–771. [CrossRef]
7. Craiu, A.; Gaczynska, M.; Akopian, T.; Gramm, C.F.; Fenteany, G.; Goldberg, A.L.; Rock, K.L. Lactacystin and clasto-lactacystin beta-lactone modify multiple proteasome beta-subunits and inhibit intracellular protein degradation and major histocompatibility complex class I antigen presentation. *J. Biol. Chem.* **1997**, *272*, 13437–13445. [CrossRef]
8. Glickman, M.H.; Ciechanover, A. The ubiquitin-proteasome proteolytic pathway: Destruction for the sake of construction. *Physiol. Rev.* **2002**, *82*, 373–428. [CrossRef]
9. Ciechanover, A.; Brundin, P. The ubiquitin proteasome system in neurodegenerative diseases: Sometimes the chicken, sometimes the egg. *Neuron* **2003**, *40*, 427–446. [CrossRef]
10. Schwartz, A.L.; Ciechanover, A. Targeting proteins for destruction by the ubiquitin system: Implications for human pathobiology. *Annu Rev. Pharmacol. Toxicol.* **2009**, *49*, 73–96. [CrossRef]
11. Unno, M.; Mizushima, T.; Morimoto, Y.; Tomisugi, Y.; Tanaka, K.; Yasuoka, N.; Tsukihara, T. The structure of the mammalian 20S proteasome at 2.75 A resolution. *Structure* **2002**, *10*, 609–618. [CrossRef]
12. Demartino, G.N.; Gillette, T.G. Proteasomes: Machines for all reasons. *Cell* **2007**, *129*, 659–662. [CrossRef] [PubMed]
13. Kisselev, A.F.; Callard, A.; Goldberg, A.L. Importance of the different proteolytic sites of the proteasome and the efficacy of inhibitors varies with the protein substrate. *J. Biol. Chem.* **2006**, *281*, 8582–8590. [CrossRef] [PubMed]
14. Sacco, A.; Aujay, M.; Morgan, B.; Azab, A.K.; Maiso, P.; Liu, Y.; Zhang, Y.; Azab, F.; Ngo, H.T.; Issa, G.C.; et al. Carfilzomib-dependent selective inhibition of the chymotrypsin-like activity of the proteasome leads to antitumor activity in Waldenstrom's Macroglobulinemia. *Clin. Cancer Res.* **2011**, *17*, 1753–1764. [CrossRef]
15. Goldberg, A.L. Development of proteasome inhibitors as research tools and cancer drugs. *J. Cell. Biol.* **2012**, *199*, 583–588. [CrossRef]
16. Kim, H.M.; Yu, Y.; Cheng, Y. Structure characterization of the 26S proteasome. *Biochim. Biophys. Acta* **2011**, *1809*, 67–79. [CrossRef]
17. Kisselev, A.F.; van der Linden, W.A.; Overkleeft, H.S. Proteasome inhibitors: An expanding army attacking a unique target. *Chem. Biol.* **2012**, *19*, 99–115. [CrossRef]

18. Groll, M.; Ditzel, L.; Lowe, J.; Stock, D.; Bochtler, M.; Bartunik, H.D.; Huber, R. Structure of 20S proteasome from yeast at 2.4 A resolution. *Nature* **1997**, *386*, 463–471. [CrossRef]
19. Weissman, A.M.; Shabek, N.; Ciechanover, A. The predator becomes the prey: Regulating the ubiquitin system by ubiquitylation and degradation. *Nat. Rev. Mol. Cell. Biol.* **2011**, *12*, 605–620. [CrossRef]
20. Manasanch, E.E.; Orlowski, R.Z. Proteasome inhibitors in cancer therapy. *Nat. Rev. Clin. Oncol.* **2017**, *14*, 417–433. [CrossRef]
21. Groll, M.; Berkers, C.R.; Ploegh, H.L.; Ovaa, H. Crystal structure of the boronic acid-based proteasome inhibitor bortezomib in complex with the yeast 20S proteasome. *Structure* **2006**, *14*, 451–456. [CrossRef] [PubMed]
22. Adams, J.; Behnke, M.; Chen, S.; Cruickshank, A.A.; Dick, L.R.; Grenier, L.; Klunder, J.M.; Ma, Y.T.; Plamondon, L.; Stein, R.L. Potent and selective inhibitors of the proteasome: Dipeptidyl boronic acids. *Bioorg. Med. Chem. Lett.* **1998**, *8*, 333–338. [CrossRef]
23. Dou, Q.P.; Zonder, J.A. Overview of proteasome inhibitor-based anti-cancer therapies: Perspective on bortezomib and second generation proteasome inhibitors versus future generation inhibitors of ubiquitin-proteasome system. *Curr. Cancer Drug Targets* **2014**, *14*, 517–536. [CrossRef] [PubMed]
24. Chen, D.; Frezza, M.; Schmitt, S.; Kanwar, J.; Dou, Q.P. Bortezomib as the first proteasome inhibitor anticancer drug: Current status and future perspectives. *Curr. Cancer Drug Targets* **2011**, *11*, 239–253. [CrossRef]
25. Britton, M.; Lucas, M.M.; Downey, S.L.; Screen, M.; Pletnev, A.A.; Verdoes, M.; Tokhunts, R.A.; Amir, O.; Goddard, A.L.; Pelphrey, P.M.; et al. Selective inhibitor of proteasome's caspase-like sites sensitizes cells to specific inhibition of chymotrypsin-like sites. *Chem. Biol.* **2009**, *16*, 1278–1289. [CrossRef]
26. Screen, M.; Britton, M.; Downey, S.L.; Verdoes, M.; Voges, M.J.; Blom, A.E.; Geurink, P.P.; Risseeuw, M.D.; Florea, B.I.; van der Linden, W.A.; et al. Nature of pharmacophore influences active site specificity of proteasome inhibitors. *J. Biol. Chem.* **2010**, *285*, 40125–40134. [CrossRef]
27. Mirabella, A.C.; Pletnev, A.A.; Downey, S.L.; Florea, B.I.; Shabaneh, T.B.; Britton, M.; Verdoes, M.; Filippov, D.V.; Overkleeft, H.S.; Kisselev, A.F. Specific cell-permeable inhibitor of proteasome trypsin-like sites selectively sensitizes myeloma cells to bortezomib and carfilzomib. *Chem. Biol.* **2011**, *18*, 608–618. [CrossRef]
28. Parlati, F.; Lee, S.J.; Aujay, M.; Suzuki, E.; Levitsky, K.; Lorens, J.B.; Micklem, D.R.; Ruurs, P.; Sylvain, C.; Lu, Y.; et al. Carfilzomib can induce tumor cell death through selective inhibition of the chymotrypsin-like activity of the proteasome. *Blood* **2009**, *114*, 3439–3447. [CrossRef]
29. Beck, P.; Dubiella, C.; Groll, M. Covalent and non-covalent reversible proteasome inhibition. *Biol. Chem.* **2012**, *393*, 1101–1120. [CrossRef]
30. Rock, K.L.; York, I.A.; Saric, T.; Goldberg, A.L. Protein degradation and the generation of MHC class I-presented peptides. *Adv. Immunol.* **2002**, *80*, 1–70.
31. Micale, N.; Scarbaci, K.; Troiano, V.; Ettari, R.; Grasso, S.; Zappala, M. Peptide-based proteasome inhibitors in anticancer drug design. *Med. Res. Rev.* **2014**, *34*, 1001–1069. [CrossRef] [PubMed]
32. Harer, S.L.; Bhatia, M.S.; Bhatia, N.M. Proteasome inhibitors mechanism; source for design of newer therapeutic agents. *J. Antibiot.* **2012**, *65*, 279–288. [CrossRef] [PubMed]
33. Borissenko, L.; Groll, M. 20S proteasome and its inhibitors: Crystallographic knowledge for drug development. *Chem. Rev.* **2007**, *107*, 687–717. [CrossRef] [PubMed]
34. Huber, E.M.; Groll, M. Inhibitors for the immuno- and constitutive proteasome: Current and future trends in drug development. *Angew. Chem. Int. Ed. Engl.* **2012**, *51*, 8708–8720. [CrossRef]
35. Han, L.Q.; Yuan, X.; Wu, X.Y.; Li, R.D.; Xu, B.; Cheng, Q.; Liu, Z.M.; Zhou, T.Y.; An, H.Y.; Wang, X.; et al. Urea-containing peptide boronic acids as potent proteasome inhibitors. *Eur. J. Med. Chem.* **2017**, *125*, 925–939. [CrossRef] [PubMed]
36. Ruschak, A.M.; Slassi, M.; Kay, L.E.; Schimmer, A.D. Novel proteasome inhibitors to overcome bortezomib resistance. *J. Natl. Cancer Inst.* **2011**, *103*, 1007–1017. [CrossRef]
37. Schrader, J.; Henneberg, F.; Mata, R.A.; Tittmann, K.; Schneider, T.R.; Stark, H.; Bourenkov, G.; Chari, A. The inhibition mechanism of human 20S proteasomes enables next-generation inhibitor design. *Science* **2016**, *353*, 594–598. [CrossRef]
38. Stein, M.L.; Cui, H.; Beck, P.; Dubiella, C.; Voss, C.; Kruger, A.; Schmidt, B.; Groll, M. Systematic comparison of peptidic proteasome inhibitors highlights the alpha-ketoamide electrophile as an auspicious reversible lead motif. *Angew. Chem. Int. Ed. Engl.* **2014**, *53*, 1679–1683. [CrossRef]
39. Grawert, M.A.; Gallastegui, N.; Stein, M.; Schmidt, B.; Kloetzel, P.M.; Huber, R.; Groll, M. Elucidation of the alpha-keto-aldehyde binding mechanism: A lead structure motif for proteasome inhibition. *Angew. Chem. Int. Ed. Engl.* **2011**, *50*, 542–544. [CrossRef]
40. Groll, M.; Nazif, T.; Huber, R.; Bogyo, M. Probing structural determinants distal to the site of hydrolysis that control substrate specificity of the 20S proteasome. *Chem. Biol.* **2002**, *9*, 655–662. [CrossRef]
41. Bota, D.A.; Mason, W.; Kesari, S.; Magge, R.; Winograd, B.; Elias, I.; Reich, S.D.; Levin, N.; Trikha, M.; Desjardins, A. Marizomib alone or in combination with bevacizumab in patients with recurrent glioblastoma: Phase I/II clinical trial data. *Neurooncol. Adv.* **2021**, *3*, vdab142. [CrossRef] [PubMed]
42. Imbach, P.; Lang, M.; Garcia-Echeverria, C.; Guagnano, V.; Noorani, M.; Roesel, J.; Bitsch, F.; Rihs, G.; Furet, P. Novel beta-lactam derivatives: Potent and selective inhibitors of the chymotrypsin-like activity of the human 20S proteasome. *Bioorg. Med. Chem. Lett.* **2007**, *17*, 358–362. [CrossRef] [PubMed]

43. Rydzewski, R.M.; Burrill, L.; Mendonca, R.; Palmer, J.T.; Rice, M.; Tahilramani, R.; Bass, K.E.; Leung, L.; Gjerstad, E.; Janc, J.W.; et al. Optimization of subsite binding to the beta5 subunit of the human 20S proteasome using vinyl sulfones and 2-keto-1,3,4-oxadiazoles: Syntheses and cellular properties of potent, selective proteasome inhibitors. *J. Med. Chem.* **2006**, *49*, 2953–2968. [CrossRef] [PubMed]
44. Ettari, R.; Bonaccorso, C.; Micale, N.; Heindl, C.; Schirmeister, T.; Calabro, M.L.; Grasso, S.; Zappala, M. Development of novel peptidomimetics containing a vinyl sulfone moiety as proteasome inhibitors. *ChemMedChem* **2011**, *6*, 1228–1237. [CrossRef] [PubMed]
45. Van der Linden, W.A.; Willems, L.I.; Shabaneh, T.B.; Li, N.; Ruben, M.; Florea, B.I.; van der Marel, G.A.; Kaiser, M.; Kisselev, A.F.; Overkleeft, H.S. Discovery of a potent and highly beta1 specific proteasome inhibitor from a focused library of urea-containing peptide vinyl sulfones and peptide epoxyketones. *Org. Biomol. Chem.* **2012**, *10*, 181–194. [CrossRef]
46. Baldisserotto, A.; Destro, F.; Vertuani, G.; Marastoni, M.; Gavioli, R.; Tomatis, R. N-terminal-prolonged vinyl ester-based peptides as selective proteasome beta1 subunit inhibitors. *Bioorg. Med. Chem.* **2009**, *17*, 5535–5540. [CrossRef]
47. Clerc, J.; Schellenberg, B.; Groll, M.; Bachmann, A.S.; Huber, R.; Dudler, R.; Kaiser, M. Convergent Synthesis and Biological Evaluation of Syringolin A and Derivatives as Eukaryotic 20S Proteasome Inhibitors. *Eur. J. Org. Chem.* **2010**, *2010*, 3991–4003. [CrossRef]
48. Groll, M.; Gallastegui, N.; Marechal, X.; Le Ravalec, V.; Basse, N.; Richy, N.; Genin, E.; Huber, R.; Moroder, L.; Vidal, J.; et al. 20S proteasome inhibition: Designing noncovalent linear peptide mimics of the natural product TMC-95A. *ChemMedChem* **2010**, *5*, 1701–1705. [CrossRef]
49. Genin, E.; Reboud-Ravaux, M.; Vidal, J. Proteasome inhibitors: Recent advances and new perspectives in medicinal chemistry. *Curr. Top. Med. Chem.* **2010**, *10*, 232–256. [CrossRef]
50. Mishto, M.; Bellavista, E.; Santoro, A.; Stolzing, A.; Ligorio, C.; Nacmias, B.; Spazzafumo, L.; Chiappelli, M.; Licastro, F.; Sorbi, S.; et al. Immunoproteasome and LMP2 polymorphism in aged and Alzheimer's disease brains. *Neurobiol. Aging* **2006**, *27*, 54–66. [CrossRef]
51. Kohno, J.; Koguchi, Y.; Nishio, M.; Nakao, K.; Kuroda, M.; Shimizu, R.; Ohnuki, T.; Komatsubara, S. Structures of TMC-95A-D: Novel proteasome inhibitors from Apiospora montagnei sacc. TC 1093. *J. Org. Chem.* **2000**, *65*, 990–995. [CrossRef] [PubMed]
52. Kaiser, M.; Groll, M.; Renner, C.; Huber, R.; Moroder, L. The core structure of TMC-95A is a promising lead for reversible proteasome inhibition. *Angew. Chem. Int. Ed. Engl.* **2002**, *41*, 780–783. [CrossRef]
53. Song, R.; Qiao, W.; He, J.; Huang, J.; Luo, Y.; Yang, T. Proteases and Their Modulators in Cancer Therapy: Challenges and Opportunities. *J. Med. Chem.* **2021**, *64*, 2851–2877. [CrossRef] [PubMed]
54. Singh, G.S. Synthetic Aziridines in Medicinal Chemistry: A Mini-Review. *Mini Rev. Med. Chem.* **2016**, *16*, 892–904. [CrossRef] [PubMed]
55. Vega-Perez, J.M.; Palo-Nieto, C.; Vega-Holm, M.; Gongora-Vargas, P.; Calderon-Montano, J.M.; Burgos-Moron, E.; Lopez-Lazaro, M.; Iglesias-Guerra, F. Aziridines from alkenyl-beta-D-galactopyranoside derivatives: Stereoselective synthesis and in vitro selective anticancer activity. *Eur. J. Med. Chem.* **2013**, *70*, 380–392. [CrossRef] [PubMed]
56. Ielo, L.; Touqeer, S.; Roller, A.; Langer, T.; Holzer, W.; Pace, V. Telescoped, Divergent, Chemoselective C1 and C1-C1 Homologation of Imine Surrogates: Access to Quaternary Chloro- and Halomethyl-Trifluoromethyl Aziridines. *Angew. Chem. Int. Edit.* **2019**, *58*, 2479–2484. [CrossRef]
57. Miele, M.; Citarella, A.; Langer, T.; Urban, E.; Zehl, M.; Holzer, W.; Ielo, L.; Pace, V. Chemoselective Homologation-Deoxygenation Strategy Enabling the Direct Conversion of Carbonyls into (n+1)-Halomethyl-Alkanes. *Org. Lett.* **2020**, *22*, 7629–7634. [CrossRef]
58. Citarella, A.; Gentile, D.; Rescifina, A.; Piperno, A.; Mognetti, B.; Gribaudo, G.; Sciortino, M.T.; Holzer, W.; Pace, V.; Micale, N. Pseudo-Dipeptide Bearing α,α-Difluoromethyl Ketone Moiety as Electrophilic Warhead with Activity against Coronaviruses. *Int. J. Mol. Sci.* **2021**, *22*, 1398. [CrossRef]
59. Citarella, A.; Micale, N. Peptidyl Fluoromethyl Ketones and Their Applications in Medicinal Chemistry. *Molecules* **2020**, *25*, 4031. [CrossRef]
60. Miele, M.; Citarella, A.; Micale, N.; Holzer, W.; Pace, V. Direct and Chemoselective Synthesis of Tertiary Difluoroketones via Weinreb Amide Homologation with a CHF2-Carbene Equivalent. *Org. Lett.* **2019**, *21*, 8261–8265. [CrossRef]
61. Trivella, D.B.; Pereira, A.R.; Stein, M.L.; Kasai, Y.; Byrum, T.; Valeriote, F.A.; Tantillo, D.J.; Groll, M.; Gerwick, W.H.; Moore, B.S. Enzyme inhibition by hydroamination: Design and mechanism of a hybrid carmaphycin-syringolin enone proteasome inhibitor. *Chem. Biol.* **2014**, *21*, 782–791. [CrossRef] [PubMed]
62. Scarbaci, K.; Troiano, V.; Micale, N.; Ettari, R.; Tamborini, L.; Di Giovanni, C.; Cerchia, C.; Grasso, S.; Novellino, E.; Schirmeister, T.; et al. Identification of a new series of amides as non-covalent proteasome inhibitors. *Eur. J. Med. Chem.* **2014**, *76*, 1–9. [CrossRef]
63. Troiano, V.; Scarbaci, K.; Ettari, R.; Micale, N.; Cerchia, C.; Pinto, A.; Schirmeister, T.; Novellino, E.; Grasso, S.; Lavecchia, A.; et al. Optimization of peptidomimetic boronates bearing a P3 bicyclic scaffold as proteasome inhibitors. *Eur. J. Med. Chem.* **2014**, *83*, 1–14. [CrossRef] [PubMed]
64. Micale, N.; Schirmeister, T.; Ettari, R.; Cinellu, M.A.; Maiore, L.; Serratrice, M.; Gabbiani, C.; Massai, L.; Messori, L. Selected cytotoxic gold compounds cause significant inhibition of 20S proteasome catalytic activities. *J. Inorg. Biochem.* **2014**, *141*, 79–82. [CrossRef] [PubMed]

65. Scarbaci, K.; Troiano, V.; Ettari, R.; Pinto, A.; Micale, N.; Di Giovanni, C.; Cerchia, C.; Schirmeister, T.; Novellino, E.; Lavecchia, A.; et al. Development of novel selective peptidomimetics containing a boronic acid moiety, targeting the 20S proteasome as anticancer agents. *ChemMedChem* **2014**, *9*, 1801–1816. [CrossRef] [PubMed]
66. Micale, N.; Ettari, R.; Lavecchia, A.; Di Giovanni, C.; Scarbaci, K.; Troiano, V.; Grasso, S.; Novellino, E.; Schirmeister, T.; Zappala, M. Development of peptidomimetic boronates as proteasome inhibitors. *Eur. J. Med. Chem.* **2013**, *64*, 23–34. [CrossRef]
67. Kisselev, A.F.; Goldberg, A.L. Monitoring activity and inhibition of 26S proteasomes with fluorogenic peptide substrates. *Methods Enzymol.* **2005**, *398*, 364–378.
68. Abdelfatah, S.; Bockers, M.; Asensio, M.; Kadioglu, O.; Klinger, A.; Fleischer, E.; Efferth, T. Isopetasin and S-isopetasin as novel P-glycoprotein inhibitors against multidrug-resistant cancer cells. *Phytomedicine* **2021**, *86*, 153196. [CrossRef]
69. Mahmoud, N.; Saeed, M.E.M.; Sugimoto, Y.; Klinger, A.; Fleischer, E.; Efferth, T. Putative molecular determinants mediating sensitivity or resistance towards carnosic acid tumor cell responses. *Phytomedicine* **2020**, *77*, 153271. [CrossRef]
70. O'Brien, J.; Wilson, I.; Orton, T.; Pognan, F. Investigation of the Alamar Blue (resazurin) fluorescent dye for the assessment of mammalian cell cytotoxicity. *Eur. J. Biochem.* **2000**, *267*, 5421–5426. [CrossRef]
71. Kimmig, A.; Gekeler, V.; Neumann, M.; Frese, G.; Handgretinger, R.; Kardos, G.; Diddens, H.; Niethammer, D. Susceptibility of Multidrug-Resistant Human Leukemia-Cell Lines to Human Interleukin 2-Activated Killer-Cells. *Cancer Res.* **1990**, *50*, 6793–6799.
72. Efferth, T.; Sauerbrey, A.; Olbrich, A.; Gebhart, E.; Rauch, P.; Weber, H.O.; Hengstler, J.G.; Halatsch, M.E.; Volm, M.; Tew, K.D.; et al. Molecular modes of action of artesunate in tumor cell lines. *Mol. Pharmacol.* **2003**, *64*, 382–394. [CrossRef] [PubMed]
73. Efferth, T.; Konkimalla, V.B.; Wang, Y.F.; Sauerbrey, A.; Meinhardt, S.; Zintl, F.; Mattern, J.; Volm, M. Prediction of broad spectrum resistance of tumors towards anticancer drugs. *Clin. Cancer Res.* **2008**, *14*, 2405–2412. [CrossRef] [PubMed]
74. Ghose, A.K.; Viswanadhan, V.N.; Wendoloski, J.J. A knowledge-based approach in designing combinatorial or medicinal chemistry libraries for drug discovery. 1. A qualitative and quantitative characterization of known drug databases. *J. Comb. Chem.* **1999**, *1*, 55–68. [CrossRef] [PubMed]
75. Veber, D.F.; Johnson, S.R.; Cheng, H.Y.; Smith, B.R.; Ward, K.W.; Kopple, K.D. Molecular properties that influence the oral bioavailability of drug candidates. *J. Med. Chem.* **2002**, *45*, 2615–2623. [CrossRef]
76. Baell, J.B.; Holloway, G.A. New substructure filters for removal of pan assay interference compounds (PAINS) from screening libraries and for their exclusion in bioassays. *J. Med. Chem.* **2010**, *53*, 2719–2740. [CrossRef]
77. Castoldi, L.; Holzer, W.; Langer, T.; Pace, V. Evidence and isolation of tetrahedral intermediates formed upon the addition of lithium carbenoids to Weinreb amides and *N*-acylpyrroles. *Chem. Commun.* **2017**, *53*, 9498–9501. [CrossRef]
78. Suffert, J. Simple Direct Titration of Organolithium Reagents Using *N*-Pivaloyl-o -toluidine and/or *N*-pivaloyl-o-benzylaniline. *J. Org. Chem.* **1989**, *54*, 509–510. [CrossRef]
79. Uneyama, K.; Amii, H.; Katagiri, T.; Kobayashi, T.; Hosokawa, T. A rich chemistry of fluorinated imidoyl halides. *J. Fluor.* **2005**, *126*, 165–171. [CrossRef]